JOURNAL OF SOLID STATE CHEMISTRY **128,** 93–96 (1997)
ARTICLE NO. SC967162

A New Electrochemical Doping Method Using M-β''-Al_2O_3 Ionic Conductors

Yasumichi Matsumoto

Department of Applied Chemistry, Faculty of Engineering, Kumamoto University, Kurokami 2-39-1, Kumamoto 860, Japan

Received May 2, 1996; in revised form September 17, 1996; accepted September 18, 1996

Electrochemical cation doping (M^{n+}) into oxide ceramics was carried out at low temperature (400–600°C) using the sandwich electrolysis system, (+)Ag/M-β''-Al_2O_3//oxide ceramics//M-β''-Al_2O_3/Ag(-), where M-β''-Al_2O_3 is a M^{n+} ionic conductor that blocks electron and oxygen anion migration in the system. Various cations (Na^+, K^+, Ag^+, Ca^{2+}, Sr^{2+}, Zn^{2+}) were doped together with substitution for Ba^{2+}, when the $YBa_2Cu_3O_y$ (YBCO) superconductor was used as the oxide ceramics. The doping occurred only in the grain boundaries of the ceramics at low electrolysis current or voltage. Under high current or voltage, only Ca^{2+} was doped into the bulk, while the other cations were doped into the grain boundaries together with destruction of the YBCO. Thus, this is a new method for selective cation doping into oxide ceramics, especially at the grain boundaries. © 1997 Academic Press

INTRODUCTION

Cation doping and/or substitution for a functional oxide ceramic are very important for improving its properties. In general, the doping into an oxide ceramic has been carried out using thermal diffusion of the dopants at high temperature. For example, Ag (1–3) and other transition metal cations (4, 5) are doped into $YBa_2Cu_3O_y$ (YBCO) ceramics at temperatures higher than about 900°C. In this case, the doping occurred over the entire ceramic, i.e., both in the bulk and at the grain boundaries. In the present paper, a new electrochemical cation doping method using the M-β''-Al_2O_3 ionic conductors is demonstrated. This method is very useful especially for doping only into the grain boundaries of oxide ceramics.

EXPERIMENTAL

In the present experiment, a YBCO superconductor was used as the oxide ceramics. Y_2O_3, $BaCO_3$, and CuO were used as the starting materials for the preparation of the YBCO powder. The mixture was heated at 930°C for 10 h, and then reground, followed by reheating under the same conditions. The pellet sample (thickness, 1.5 mm; surface area, 1.5 cm^2) of the YBCO was prepared by pressing the powder under 1000 Kg/cm^2 and heating at 930°C. The solid electrolytes of M-β''-Al_2O_3 (M: Na^+, K^+, Ca^{2+}, Sr^{2+}, Ag^+, Zn^{2+}) were prepared by the substitution of M in Na-β''-Al_2O_3 as previously reported (6–8). The presence of M in these electrolytes was confirmed by electron probe microanalysis (EPMA). The electrochemical doping was carried out for 1 h under constant current (≤ 1 mA) using the experimental setup schematically shown in Fig. 1. During this electrolysis, the electrochemical oxidation from Ag to Ag^+ occurs at the Ag anode, while the electrochemical reduction from M^{n+} to M occurs at the Ag cathode. The apparent contact area in the YBCO/M-β''-Al_2O_3 interface was 0.25 cm^2. The electrolysis was done at 400–600°C. After the electrolysis, the distribution state of the dopants in the cross section of the YBCO ceramics was analyzed using EPMA. The compositions and/or crystal structure of the doped samples were based on an analysis of their X-ray diffraction patterns. The resistivities of the doped YBCO samples were measured by a conventional dc four-probe method, using a 10 mA dc current. Their ac susceptibilities were also measured using an ac inductance bridge.

RESULTS AND DISCUSSION

The applied voltage increased with an increase in the electrolysis time, and was less than a few volts and few hundred volts for 0.01 mA and 1 mA, respectively. Only Ba was always observed in the cathode β''-Al_2O_3 electrolyte after the electrolysis under all conditions and was independent of the kind of dopants. This indicates that only the Ba^{2+} ion in the YBCO ceramics moves during the electrolysis. Simultaneously, it is suggested that the bond strength of Ba^{2+} in the YBCO structure is the weakest of all cations in the YBCO. In principle, the following electrochemical reactions will occur at both sides of the YBCO/M-β''-Al_2O_3 interfaces.

$$xM^{n+} + nxe^- + YBa_2Cu_3O_y \rightarrow YBa_2M_xCu_3O_y \quad \text{(anode side)}$$

0022-4596/97 $25.00

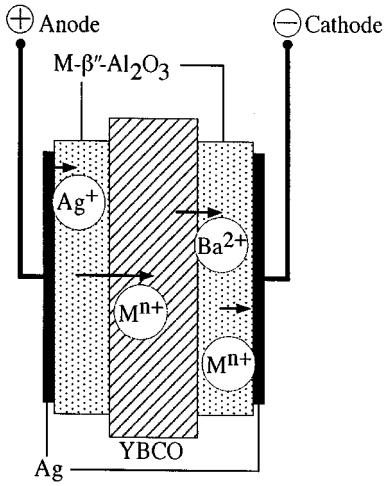

FIG. 1. Model of the electrolysis system. The total ionic migration at the interfaces during the initial stage of electrolysis is also illustrated.

$$YBa_2Cu_3O_y \rightarrow (nx/2)Ba^{2+} + nxe^- + YBa_{2-nx/2}Cu_3O_y \quad \text{(cathode side)}$$

The dopant M^{n+} in the $YBa_2M_xCu_3O_y$ will diffuse in the YBCO ceramics during the electrolysis.

After the electrolysis at a current lower than about 0.01 mA (at low applied voltage), small amounts of the dopants were detected in the grain boundaries and the pores of the YBCO ceramics, but not in the bulk. Figure 2 shows the typical distribution maps of the element and SEM micrograph of the cross section of the Sr doped YBCO at 0.01 mA. In this case, the YBCO scarcely decomposed according to the X-ray analysis, as shown in (B) of Fig. 3 which shows some typical X-ray diffraction patterns of the doped and undoped YBCO samples. Similar results were obtained for the other element doped samples at low current and/or low applied voltage. This indicates that all of the dopant cations smoothly diffuse into the grain boundaries of the YBCO ceramics together with the substitution for Ba^{2+} as illustrated in Fig. 4A. This phenomenon is due to the grain boundary ionic conduction (diffusion) that is much higher than that of the bulk for the oxide ceramics.

On the other hand, two types of phenomena were observed during the electrolysis at currents higher than about 0.01 mA (at high applied voltage). One is the grain boundary diffusion of the dopants together with the destruction of the YBCO. This occurred for all dopants except Ca^{2+}. In this case, a large amount of the dopants was observed together with impurities such as M (metal for Ag), MO (for

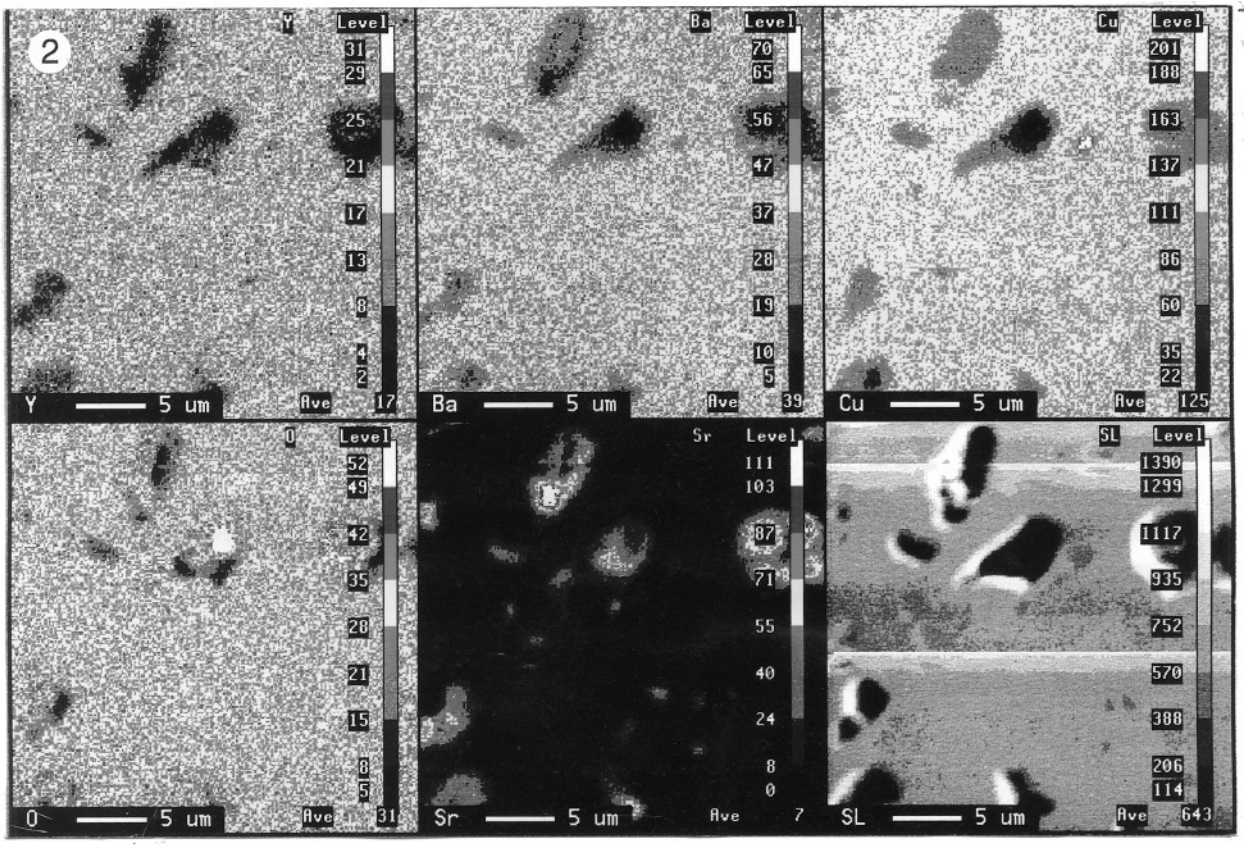

FIG. 2. Distribution maps of the element and SEM micrograph of the cross section of the Sr doped YBCO at 0.01 mA.

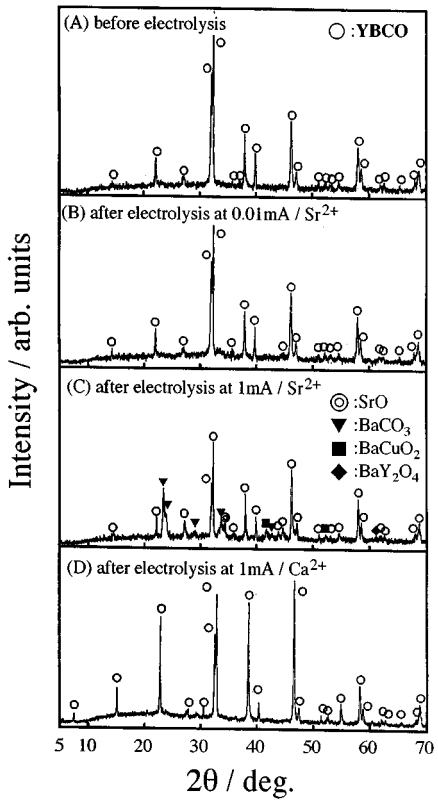

FIG. 3. Typical X-ray diffraction patterns of the doped and undoped YBCO at 600°C. (A), (B), (C), and (D) are the diffraction patterns of the undoped sample, the Sr-doped sample at 0.01 mA, the Sr-doped sample at 1 mA, and the Ca-doped sample at 1 mA, respectively.

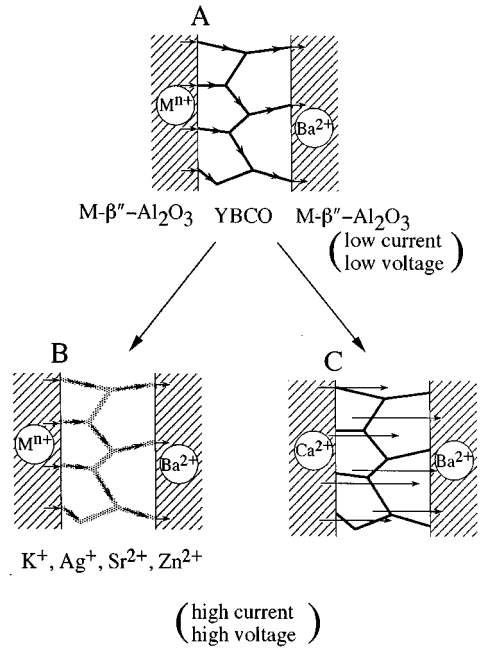

FIG. 4. Models of the diffusion paths. M^{n+} smoothly diffuses in the grain boundaries of the YBCO ceramics under low current and/or low applied bias voltage (A). Under high current and/or high applied bias voltage, M^{n+} (K^+, Ag^+, Sr^{2+}, Zn^{2+}) moves in the grain boundaries together with the destruction of the YBCO (B), while Ca^{2+} diffuses in the bulk without the same destruction (C).

Sr and Zn), CuO (for Ag and Zn), $BaCO_3$, BaY_2O_4, and $BaCuO_2$ produced by the destruction of the YBCO at the grain boundaries, as shown in Fig. 3C for the Sr-doped YBCO. These impurities will be produced by the destruction of the $YBa_2M_xCu_3O_y$ and $YBa_{2-nx/2}Cu_3O_y$ having a large x value. This doping model is illustrated in Fig. 4B.

The second phenomena is the bulk diffusion of Ca^{2+} which is very surprising. Figure 5 shows the distribution maps of the element and a SEM micrograph of the cross section of the Ca-doped YBCO at 1 mA. Ca uniformly existed over the entire bulk of the YBCO. Moreover, no destruction of YBCO occurred during the electrolysis according to the X-ray analysis as shown in Fig. 3D. That is, Ca^{2+} moves together with substitution for Ba^{2+} in the YBCO structure whose model is illustrated in Fig. 4C. The lattice constants decreased from $a = 3.81$ Å, $b = 3.89$ Å, $c = 11.68$ Å for the present pure YBCO to $a = 3.73$ Å, $b = 3.85$ Å, $c = 11.52$ Å for the Ca-doped YBCO at 1 mA, and whose composition was analyzed to be $YBa_{1.93}Ca_{0.07}Cu_3O_y$ according to the EPMA analysis. No substitution of Ca^{2+} for Ba^{2+} occurred due to heat-treatment at 600°C if no bias voltage was applied. Whether or not the bulk diffusion occurs depends on the dopants, but not Ba^{2+}, because Ba^{2+} always moves independent of the kind of dopants. Ca^{2+} will easily diffuse via the Ba^{2+} site to the YBCO structure, since its ionic size is relatively small and it has the same coordination number as Ba^{2+}.

Figure 6 shows the dependence of the resistivity on temperature for the present YBCO ceramics, which reflects both the superconducting properties of the bulk and the grain boundary. The T_c in the ac susceptibility measurement scarcely changed for the Ca-doped (bulk) and the Ag-doped (grain boundary without the destruction) YBCO samples. Therefore, a small shift in the resistive T_c and a decrease in the resistivity at room temperature for the Ag doped YBCO shown in Fig. 6C are due to the improvement in the grain boundaries by Ag (9,10).

Thus, the present method is very useful for the doping into only grain boundaries of oxide ceramics using a selective cation, if the doping is carried out under low current or low voltage. Moreover, significant cation doping into the bulk will sometimes occur for other oxide ceramics using the present method, which will simultaneously reflect the degree of the bond strength of the constituting cation in the structure. Therefore, the doping tests for other oxide ceramics are in progress.

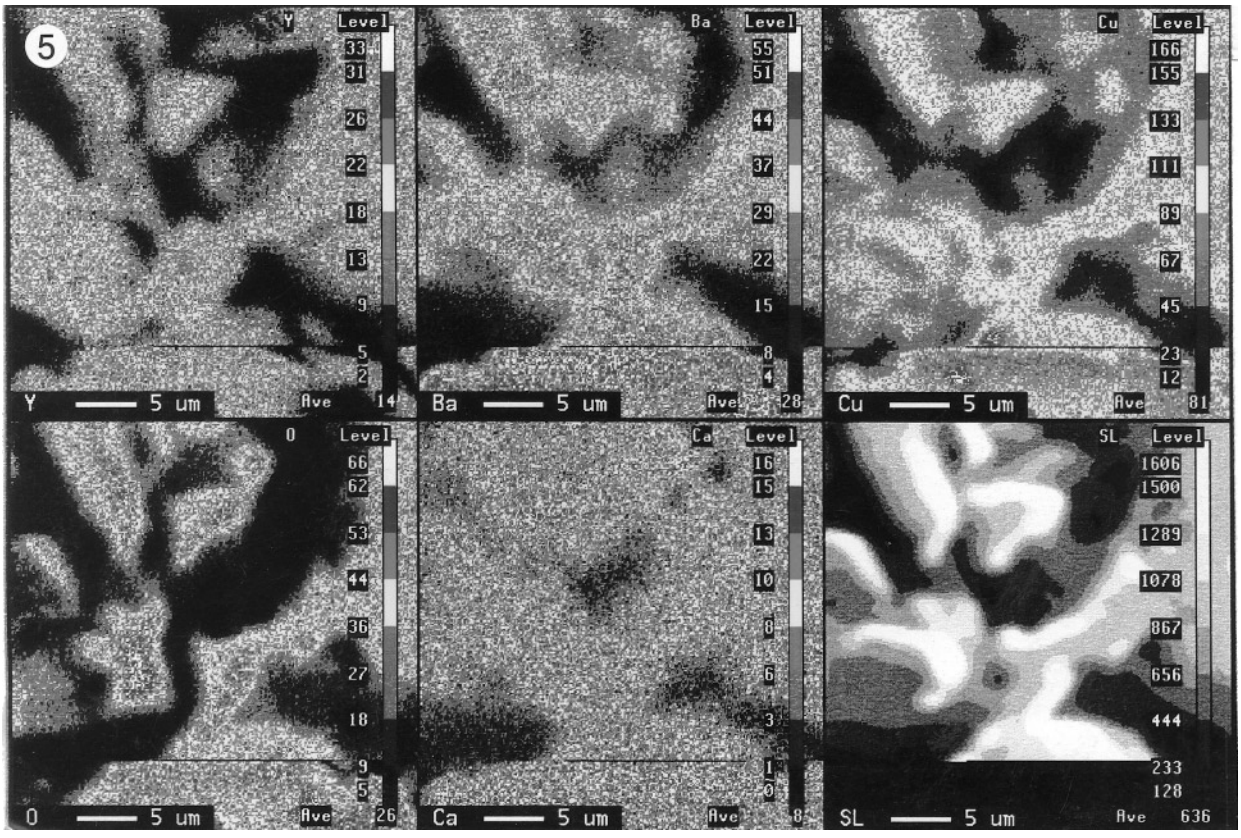

FIG. 5. Distribution maps of the element and SEM micrograph of the cross section of the Ca-doped YBCO at 1 mA.

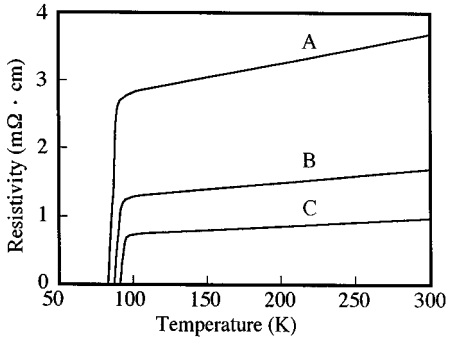

FIG. 6. Dependencies of the resistivities of the YBCO samples on temperature. The resistivity of the Ca-doped YBCO under 1 mA at 600°C (A, bulk doping) increased compared with the pure sample (B), although the T_c slightly shifted to low. The resistivity at room temperature and the T_c of the Ag-doped YBCO under 3×10^{-3} mA at 600°C (C, grain boundary doping) decreased and shifted to a higher value, respectively.

REFERENCES

1. D. Cahen, Z. Moisi, and M. Schwartz, *Mater. Res. Bull.* **22,** 1581 (1987).
2. Y. Matsumoto, T. Abe, M. Tanaka, T. Tazawa, and E. Sato, *Mater. Res. Bull.* **23,** 1241 (1988).
3. P. N. Peters, R. C. Sisk, E. W. Urban, C. Y. Huang, and M. K. Wu, *Appl. Phys. Lett.* **52,** 2066 (1988).
4. J. M. Tarascon, L. H. Greene, W. R. McKinnon, and G. W. Hull, *Phys. Rev. B*35, 7115 (1987).
5. T. Siegrist, S. Sunshine, D. W. Murphy, R. J. Cava, and S. M. Zahurak, *Phys. Rev. B* **35,** 7249 (1987).
6. M. S. Whittingham and R. A. Huggins, *J. Electrochem. Soc.* **118,** 1 (1971).
7. G. C. Farrington and B. Dunn, *Solid State Ionics* **7,** 267 (1982).
8. M. Breiter, M. M. Schreiber and B. Dunn, *Solid State Ionics* **18/19,** 658 (1986).
9. Y. Matsumoto, J. Hombo, Y. Yamaguchi, N. Nishida, and A. Chiba, *Appl. Phys. Lett.* **56,** 1585 (1990).
10. Y. Matsumoto, Y. Yamaguchi, J. Hombo, T. Hauber, and W. Gopel, *J. Solid State Chem.* **98,** 201 (1992).